Dalton Transactions

ROYAL SOCIETY OF CHEMISTRY

PAPER

View Article Online
View Journal | View Issue

Check for updates

Cite this: *Dalton Trans.*, 2025, **54**, 10883

Rapid and sensitive determination of etomidate based on colorimetric assays with a chromium(III) complex†

Leo K. B. Tam, *‡[a] Weijun Ma,‡[b] Boyang Li, ‡[b] Waygen Thor, [a] Ho-Fai Chau *[a] and Ka-Leung Wong *[a]

Received 9th April 2025,
Accepted 10th June 2025

DOI: 10.1039/d5dt00849b

rsc.li/dalton

Vaping etomidate is currently a red-hot social issue where the drug abuse problem has led to health concerns and even reported deaths for adolescents. Therefore, a fast, sensitive, and cost-effective detection tool for etomidate is urgently needed to support law enforcement. A chromium(III) complex-based sensor, **EtoChrom**, is presented in this work as an example of a detection method for etomidate based on a colorimetric assay. This low-priced but novel sensor exhibits an eye-catching colour change from purple to yellow and a bathochromic shift in the absorption band upon etomidate binding. Thus, the result can be seen directly by the naked eye. **EtoChrom** demonstrated a high precision of up to 2 mg mL^{-1} etomidate with a low detection limit of 0.030 mg mL^{-1}, with the interference from the vape juice and saliva matrices negligible throughout the test. In real etomidate-containing vape juice analysis, **EtoChrom** can provide accurate results within 1 min, revealing its high potential to serve as an easy-to-handle and cost-effective etomidate detector for rapid on-site screening.

1. Introduction

Etomidate (ET) is an imidazole-based non-barbiturate sedative, which is ordinarily applied for anaesthesia induction and sedation in the form of injection.[1] With its strong but ultra-short inhibitory effect on the central nervous system, ET might provide short-term pleasure similar to inebriation for humans.[2] However, an overdose of ET can lead to adrenal suppression, myoclonus, respiratory depression, unconsciousness, and even death.[3,4] Recently, ET has been found to be a low-cost and easily obtainable substitute for narcotics, leading to a tremendous growth rate in criminal cases of its illegal addition to beverages and vape juice of E-cigarettes in Hong Kong and China in the last two years.[5] Consequently, in February 2025, ET and its analogues, including metomediate (MT), propoxate, and isopropoxate (iPrT), were classified as dangerous drugs in Hong Kong.[6] Hence, there is an urgent need to develop fast, selective and cost-effective ET sensors to support law enforcement.

The current reported analytical methods for ET in human or environmental samples are mainly based on high-performance liquid chromatography (HPLC) or gas chromatography (GC) equipped with a mass detector (MS).[7–9] Despite their ability to achieve highly accurate results with a remarkably low limit of detection (LOD), the requirements of long testing time, expensive and large equipment, and professional operators restrict their use under non-laboratory conditions. To overcome these limitations, Peng *et al.*[10] and Ding *et al.*[11] reported two fluorescence sensors that can recognize ET with the LOD in the nanomolar (nM) range, respectively, in 2024. However, using a fluorescence sensing strategy to detect narcotics or drugs heavily relies on the use of spectrofluorometers,[12–14] and either the portable instruments are expensive or the signal-to-background ratio is limited, significantly reducing the practical feasibility of on-site ET determination.[15] Alternatively, in 2025, the use of lateral-flow immunoassay by Qu *et al.* provided an ultra-low (ppb level) detection result for both ET and MT in human and environmental samples.[16] Yet, the preparation of monoclonal antibodies of both analytes through the development of engineered haptens was costly and time-consuming.[17] Apart from the chemical sensor, Zhang *et al.* in 2025 demonstrated the use of gold-ordered array substrate-engineered surface-enhanced Raman spectrometry to detect ET and its metab-

[a]*Department of Applied Biology and Chemical Technology, The Hong Kong Polytechnic University, Hung Hom, Hong Kong, PR China. E-mail: leo-kb.tam@polyu.edu.hk, ho-fai.chau@polyu.edu.hk, klgwong@polyu.edu.hk*

[b]*Department of Chemistry, Hong Kong Baptist University, 224 Waterloo Road, Kowloon Tong, Kowloon, Hong Kong, PR China*

†Electronic supplementary information (ESI) available: Experimental, UV-vis absorption spectra and LC/MS chromatograms. See DOI: https://doi.org/10.1039/d5dt00849b

‡These authors contributed equally.

olites in vape juice at a concentration of 50 ppm.[18] Nevertheless, fabrication of the gold array required tedious and apparatus-assisted synthesis. The benefits and drawbacks of recent and representative detection methods of ET are compared and summarised in Table S2.†

Notably, colorimetric analysis, particularly colour variation upon metal ion chelation,[19] is the most frequently employed method for on-site inspection of psychoactive drugs and narcotics. For example, transition metals such as Co^{2+} ions (the Dille–Koppanyi reagent for barbiturates) and Cu^{2+} ions (the Zwikker reagent for barbiturates) are commonly adopted in preliminary visual examination in the analysis of barbiturates owing to the ease of preparation and rapid reaction kinetics.[20,21] Among other transition metal ions, Cr^{3+} in the form of a $[Cr(H_2O)_6]^{3+}$ complex has drawn our attention because of the immediate and clear visual colour change from purple to greenish yellow upon the displacement of one aqua ligand by an electron-rich ligand;[22,23] the lone-pair electrons on the imidazole ring and/or the carbonyl of ET are expected to promote this rapid ligand exchange, resulting in ET-specific recognition. Besides, the common source of $[Cr(H_2O)_6]^{3+}$, chromium(III) nitrate nonahydrate $[Cr(NO_3)_3{\cdot}9H_2O]$,[24] is inexpensive.[25] However, to the best of our knowledge, the potential of applying this Cr^{3+}-based colorimetric analysis in ET detection remains unexplored, although the result can be determined instantly and directly by the naked eye.

In this work, we report an example of using the $[Cr(H_2O)_6]^{3+}$ complex to detect ET based on a colorimetric assay. As a proof of concept, **EtoChrom**, a reagent containing 10 mM $[Cr(H_2O)_6]^{3+}$ in 10% (w/v) NaCl solution, is prepared as a low-cost, rapid, sensitive and selective ET sensor which can provide both qualitative and quantitative results. The sensitivity, LOD, selectivity and stability of **EtoChrom** will be discussed along with its feasibility for on-site detection of ET.

2. Results and discussion

2.1. Molecular design and mechanistic action

Imidazole is an electron-rich field ligand relatively stronger than H_2O in the spectrochemical series (*i.e.* H_2O < NCS^- < CH_3CN < imidazole < py < NH_3).[26,27] Upon interaction of the $[Cr(H_2O)_6]^{3+}$ complex in octahedral geometry (O_h) with ET in the E-cigarette sample, a substitution reaction would occur to displace one water molecule to give $[Cr(H_2O)_5ET]^{3+}$ with the preferred dissociative mechanism.[28] Owing to the presence of a stronger field ET ligand, an immediate visual colour change from purple (*i.e.* absorption in the yellow region *ca.* 580 nm) to greenish yellow (*i.e.* absorption in the violet region *ca.* 400 nm) is expected due to the increase in crystal field splitting energy (Δ_o), resulting in a higher absorbance in the high-energy violet region and a bathochromic shift of maximum absorption wavelength according to the crystal field theory (Fig. 1a).[22,23]

To validate the key principle in the design of our ET sensor, commercially purchased $[Cr(H_2O)_6]^{3+}$ was first dissolved in deionized (DI) water to give a solution of 10 mM concentration.

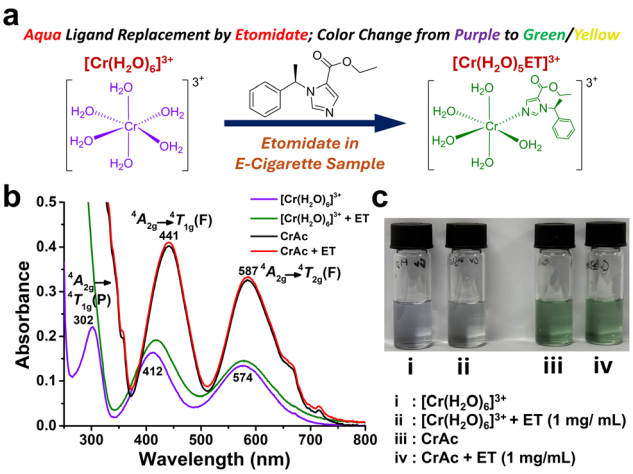

Fig. 1 (a) Schematic illustration of the ET detection mechanism of the $[Cr(H_2O)_6]^{3+}$ complex. Change in (b) UV-vis spectra and (c) colour of $[Cr(H_2O)_6]^{3+}$ and CrAc (both 10 mM) in DI water upon the addition of ET (1 mg mL^{-1}).

As a control, a 10 mM green chromium(III) acetate (CrAc) aqueous solution was also prepared. As shown in Fig. 1b, the absorption spectra of both chromium aqua and acetate complexes exhibited three major absorption bands attributed to the three spin-allowed d–d transitions for the O_h complex in a d_3 system, $^4A_{2g} \rightarrow {}^4T_{1g}(P)$ (*ca.* 300 nm), $^4A_{2g} \rightarrow {}^4T_{1g}(F)$ (*ca.* 420 nm), and $^4A_{2g} \rightarrow {}^4T_{2g}(F)$ (*ca.* 580 nm), respectively, which were essentially the same as those reported.[23,29] The letters F and P are symbols describing the total orbital angular momentum (L = 1 or 3) of the excited state terms for clarity, respectively, in which their orbital angular momentum may be different from the free ion ground state (^4F) of the d^3 system.[22] Upon the addition of 1 mg mL^{-1} of ET with 1 min shaking, while the absorption spectrum of the CrAc showed negligible change, bathochromic shifts of maximum absorption wavelength (λ_{abs}) for both the $^4A_{2g} \rightarrow {}^4T_{1g}(F)$ transition from 412 to 416 nm and the $^4A_{2g} \rightarrow {}^4T_{2g}(F)$ transition from 574 to 577 nm were observed in the case of the chromium aqua complex [Fig. 1b and S1a†], leading to a gradient colour change from purple to greenish yellow (Fig. 1c). In addition, the absorbance for $^4A_{2g} \rightarrow {}^4T_{1g}(F)$ transition increased from 0.16 to 0.19 (Fig S1b†). These results supported the ET detecting properties of the $[Cr(H_2O)_6]^{3+}$ complex as a colorimetric sensor.

2.2. Optimisation of detection conditions

The effects of pH, medium, concentration, and reaction time were further investigated for the optimal ET detection conditions with the $[Cr(H_2O)_6]^{3+}$ complex. To study the pH effect, the absorption spectra of 10 mM $[Cr(H_2O)_6]^{3+}$ aqueous solution were recorded with the pH adjusted from 1 to 11. As shown in Fig. S2,† under acidic conditions (pH 1.0 and 3.0), while the λ_{abs} for three transition bands remained unchanged, their absorbance was slightly reduced compared with that of aqueous $[Cr(H_2O)_6]^{3+}$ solution dissolved in DI water. At pH 7.0, a small amount of pale green suspension was noticed, likely

chromium(III) hydroxide [$Cr(OH)_3$]. Meanwhile, $CrOH^{2+}$ and/or $[Cr(OH)_2]^+$ complexes were likely formed, which might alter the absorption spectrum of the mixture.[30] At pH 9.0, a significant amount of pale green solid precipitated from the solution. It is well known that the presence of precipitates in the cuvette causes radiation scattering, which noticeably increases absorbance.[31] Interestingly, at pH 11.0, the pale green precipitate redissolved in this alkaline environment, which changed the absorption profile as $[Cr(OH_4)]^-$ was expected to be the predominant complex in the solution.[30] In particular, at pH 5.0, the absorption profile almost overlapped with that of the$[Cr(H_2O)_6]^{3+}$ aqueous solution, suggesting that this pH value provided minimum interference. The buffer solution can resist pH change and thereby the spectral properties of the $[Cr(H_2O)_6]^{3+}$ complex were analysed in phosphate-buffered saline (PBS) and sodium acetate (NaAc) at pH 5.0 at different concentrations (Fig. S3a†). At 100 mM, absorption bands at 411 nm showed a bathochromic shift to 420 and 425 nm in PBS and NaAc, respectively (Fig. S3b†). When the concentration of the buffer was reduced to 10 or 1 mM, the change in λ_{abs} became marginal but the absorbance was still remarkably higher than that in DI water (Fig. S3c†), implying that the use of buffer solution was not suitable. Instead, we dissolved the $[Cr(H_2O)_6]^{3+}$ complex in 10% (w/v) NaCl solution to minimize biodegradation for prolonged storage, since the high salt concentration can effectively inhibit the growth of bacteria and viruses.[32] The absorption spectrum of $[Cr(H_2O)_6]^{3+}$ in this medium was then measured and found to be very similar to that recorded in DI water (Fig. 2a).

To further identify the optimal concentration of $[Cr(H_2O)_6]^{3+}$ in this formulation for ET detection, 1 mg mL^{-1} ET was added to the solution with three different concentrations of $[Cr(H_2O)_6]^{3+}$, and the results are depicted in Fig. S4.† It was found that the purple colour at 100 mM was too intense for a positive result reading, while it was difficult to distinguish the colour between the transparent 1 mM testing solution and the ET-chelated mixture by the naked eye. Thus, 10 mM $[Cr(H_2O)_6]^{3+}$ in 10% (w/v) NaCl solution at pH 5.0 (**EtoChrom**) was chosen in the subsequent experiments. The optimal result reading time for **EtoChrom** was also studied by the change in the absorption profile upon the addition of 1 mg mL^{-1} ET with different shaking times. As shown in Fig. S5,† the λ_{abs} of $^4A_{2g} \rightarrow {}^4T_{1g}(F)$ transition increased gradually to 417 nm and reached a plateau at around 1 min. Meanwhile, the absorbance of this band sharply increased to 0.24 in the first 10 s and eventually reduced and stabilized at *ca.* 0.19 after 1 min. The summarized results in Fig. 2b suggest that **EtoChrom** can serve as a rapid ET sensor, which is attributed to the rapid equilibrium achieved in Cr-ET complexation within 1 min.

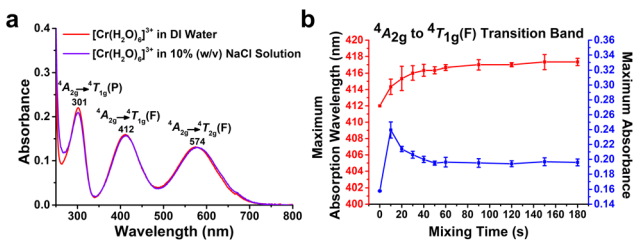

Fig. 2 (a) UV-vis spectra of $[Cr(H_2O)_6]^{3+}$ (10 mM) in DI water or 10% (w/v) NaCl solution. (b) Change in λ_{abs} and absorbance for the $^4A_{2g} \rightarrow {}^4T_{1g}(F)$ transition of **EtoChrom** (10 mM) upon the addition of ET (1 mg mL^{-1}) over a period of 3 min.

2.3. Stability of EtoChrom

The stability of **EtoChrom** was then examined by monitoring the change in the absorption spectrum of **EtoChrom** (10 mM) at room temperature over a period of 90 days (Fig. 3a). It can be seen that the changes in both λ_{abs} and absorbance for $^4A_{2g} \rightarrow {}^4T_{1g}(F)$ and $^4A_{2g} \rightarrow {}^4T_{2g}(F)$ bands were inconsequential throughout the whole period (Fig. S6a and b†). To further understand the ET detection properties of **EtoChrom** stored for a long time, a detection assay was performed with **EtoChrom** incubated with ET (1 mg mL^{-1}) for 28, 56, and 90 days. As shown in Fig. S7,† the absorption spectra at these time points were comparable to those recorded at day 0. All of these results confirmed the high stability and retained ET recognition ability of **EtoChrom** over a period of storage.

2.4. Sensitivity of EtoChrom

To investigate the correlation between the λ_{abs} and absorbance of **EtoChrom** and the concentration of ET, the absorption spectra of **EtoChrom** upon the addition of ET from 0 to 40 mg mL^{-1} with 1 min of shaking were recorded (Fig. 3b). As expected, a bathochromic shift in λ_{abs} and enhanced absorbance can be observed for both the $^4A_{2g} \rightarrow {}^4T_{1g}(F)$ and $^4A_{2g} \rightarrow {}^4T_{2g}(F)$ transition bands, along with a notable visual colour change from purple to greenish yellow when the concentration of ET increased (Fig. 3c). As shown in Fig. 3d and S8a–c,† the λ_{abs} of the $^4A_{2g} \rightarrow {}^4T_{1g}(F)$ band exhibited a good linear relationship with the concentration of ET among three other parameters (*i.e.* λ_{abs} of $^4A_{2g} \rightarrow {}^4T_{2g}(F)$ and the absorbance of two transition bands) within 2 mg mL^{-1}, indicating the colorimetric nature of **EtoChrom** in ET sensing. However, when the ET concentration was >2 mg mL^{-1}, the λ_{abs} at 424 nm reached a plateau and it is believed that the concentration was saturated and precipitation of ET was observed, losing the linear relationship with the λ_{abs} or absorbance. The LOD was also determined to be 0.030 mg mL^{-1}, while the colour change can be visualized by the human eye at *ca.* 1 mg mL^{-1}.

2.5. Selectivity of EtoChrom

It is important to understand if **EtoChrom** is specific toward etomidate and unaffected by other common analytes in the matrices during the analysis. Since our target is to develop a specific on-site ET detection means, various potential interfering species, including glycerol (EG), propylene glycol (PG), flavouring chemicals and nicotine in the vape juice,[33] and electrolytes (*i.e.* Na^+, K^+, Ca^{2+}, Mg^{2+}, Cl^-, HCO_3^-, PO_4^{2-}), enzymes and proteins in the saliva,[34] were treated with **EtoChrom** and the changes in the absorption spectra were monitored. To simplify the assay, 20 mmol L^{-1} $NaHCO_3$, 30 mmol mL^{-1} KCl,

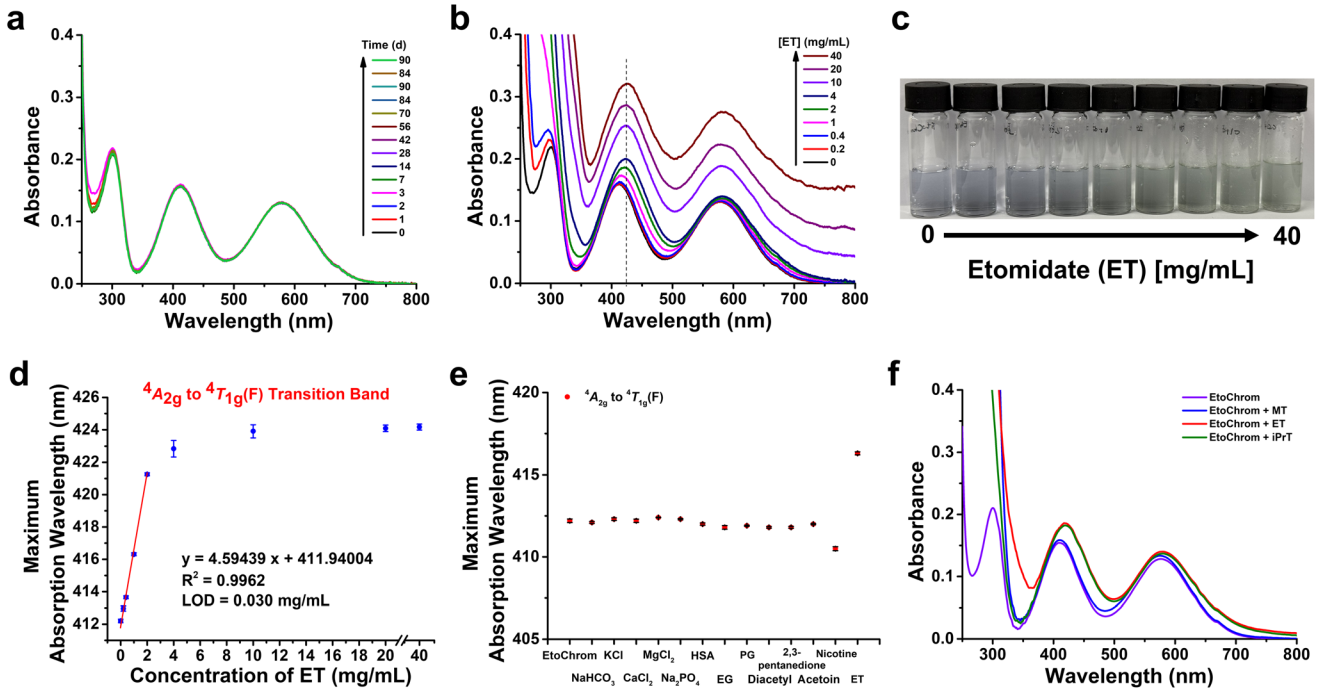

Fig. 3 Change in UV-vis spectra of **EtoChrom** (10 mM) (a) over a period of 90 days, (b) upon addition of different concentrations of ET (from 0 to 40 mg mL^{-1}), and (f) upon incubation with ET, MT, or iPrT (all at 10 mg mL^{-1}) after shaking for 1 min. (c) Change in colour of **EtoChrom** (10 mM) upon the addition of ET from 0 to 40 mg mL^{-1}. (d) The relationship between the λ_{abs} of the $^4A_{2g} \rightarrow {}^4T_{1g}(F)$ transition band of **EtoChrom** (10 mM) and the concentration of ET. (e) λ_{abs} of the $^4A_{2g} \rightarrow {}^4T_{2g}(F)$ transition band of **EtoChrom** (10 mM) after treatment with ET or different potential interfering species in the vape juice and saliva matrices with the corresponding concentrations. Data are expressed as the mean ± standard derivation (SD) of three independent experiments.

2.5 mmol L^{-1} $CaCl_2$, 0.25 mmol L^{-1} $MgCl_2$, and 30 mmol Na_2PO_4 were tested in this study while 2 mg mL^{-1} of human serum albumin (HSA) was used to mimic the total amount of enzymes and proteins, making both ion and protein concentrations similar to those in the saliva of a normal adult.[34] Because of the numerous flavours of E-cigarettes available commercially, three common and representative flavouring chemicals found in vape juice, namely diacetyl, 2,3-pentanedione, and acetoin (all 500 μg mL^{-1}), were examined in this assay.[35] In addition, the concentration of nicotine to be examined was 18 mg mL^{-1}, which is similar to the typical content of nicotine in commercially available vape juice (*i.e.* 1.8%). As shown in Fig. 3e, the change in λ_{abs} of the $^4A_{2g} \rightarrow {}^4T_{1g}(F)$ band was negligible after treatment with most species, except for nicotine, which showed a slightly hypsochromic shift for 2 nm. It is noteworthy that the absorbance at *ca.* 412 nm was higher in the cases of PO_4^{2-} and nicotine, with the difference being marginal for the former but considerable for the latter (Fig. S9†).

Therefore, the absorption spectrum of **EtoChrom** was recorded and subjected to comparison in the presence of nicotine (18 mg mL^{-1}) and ET (1 mg mL^{-1}) (Fig. S10†). Interestingly, the absorption features and change in λ_{abs} of the $^4A_{2g} \rightarrow {}^4T_{1g}(F)$ band of **EtoChrom** upon addition of nicotine and ET were similar to those for ET addition only. Furthermore, **EtoChrom** was incubated with three ratios of PG/EG [*i.e.* 6 : 4, 7 : 3, 8 : 2 (v/v)] that mimic commercial vape juice to understand its compatibility in this fundamental matrix for future real sample analysis.[36] Similar to the individual components, the absorption spectra of **EtoChrom** in all of these ratios remained almost unchanged, which suggests that our probe is inert to the major composition of vape juice in common formulations (Fig. S11†). All of the above results reveal that the bathochromic change in λ_{abs} and yellow colour formation by **EtoChrom** were highly specific to ET in the presence of the aforementioned interfering species.

The performance of **EtoChrom** with MT and iPrT (all at 1 mg mL^{-1}) was also examined because of the growing trend of the illegal addition of these ET analogues to vape juice to avoid the detection of ET.[37] Fig. 3f shows that the absorption spectra of **EtoChrom** were commensurate in the presence of ET or iPrT, while the change in λ_{abs} with MT was minimal, which might be attributed to the electron donating effect of the substituents.

Still, **EtoChrom** has the potential to recognize some other analogues of ET with a similar structure, implying its high capability to recognize illegally added ET derivatives in actual scenarios.

2.6. Calculation for etomidate–EtoChrom binding

In light of the concerns about the binding geometry between ET and **EtoChrom**, computational modelling and calculation

were employed using density functional theory (DFT) with the PBE0/def2-SVP level of theory to stimulate the optimized structure of the ET–**EtoChrom** complex.[38,39] There are three possible binding modes between the Cr^{3+} ion and the ET ligand, including (1) monodentate N-coordination with the imidazole ring; (2) monodentate C=O coordination with the ester moiety; and (3) bidentate N– and C=O coordination. As shown in Fig. 4a, the change in the single point energy (Δ_{SPE}) with reference to $[Cr(H_2O)_6]^{3+}$ for N-coordination (−32.90 kcal mol^{-1}) was calculated to be much lower than that of C=O coordination (−17.94 kcal mol^{-1}), suggesting that the ET ligand with N-coordination to the Cr^{3+} ion is preferred. Nonetheless, bidentate chelation was unlikely to be seen due to the steric hindrance and the large distance between the two binding sites (Fig. S12†). For the number of ligands coordinated onto **EtoChrom**, the calculated Δ_{SPE} of the bi-coordinated complex (−33.64 kcal mol^{-1}) was marginally lower than that of the mono-coordinated complex (−32.90 kcal mol^{-1}) (Fig. 4b). However, with reference to our experimental results given in Fig. 3d, the maximum concentration of ET with a good linear relationship detected by 10 mM **EtoChrom** was 2 mg mL^{-1} (*i.e.* 8.2 mM), while ET precipitation was observed at >4 mg mL^{-1} (*i.e.* 16.4 mM), revealing that the bi-coordination was kinetically not favoured due to the ET solubility. Hence, we believe that a 1 : 1 binding between ET and **EtoChrom** dominated in the reaction mixture although the energy of the bi-coordinated complex is lower than that of the mono-coordinated complex. All the above results suggest a strong, monodentate, and mono-coordinated binding between the Cr^{3+} ion and the ET ligand, which is consistent with our above experimental results.

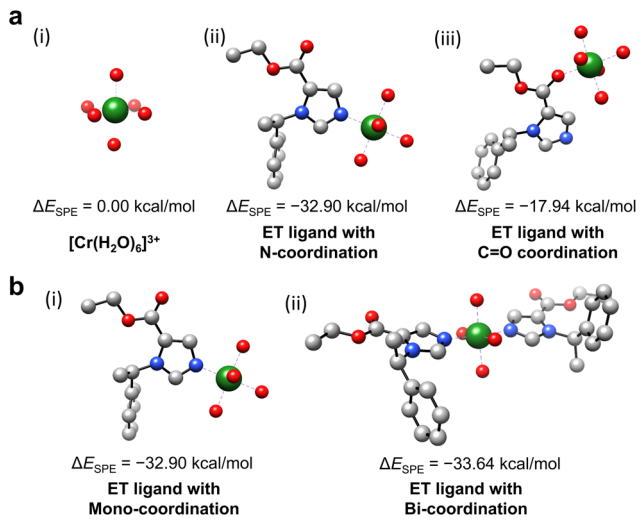

Fig. 4 (a) The optimized structures of (i) $[Cr(H_2O)_6]^{3+}$, (ii) the ET ligand with N-coordination, and (iii) the ET ligand with C=O coordination. The relative energy compared to $[Cr(H_2O)_6]^{3+}$ demonstrates a more stable conformation when coordinated on the N atom of imidazole. (b) The optimized (i) mono- and (ii) bi-ET coordinated structures and the relative energy compared to $[Cr(H_2O)_6]^{3+}$. Green: Cr; grey: C; red: O; and blue: N. Hydrogens are omitted for clarity.

Table 1 Concentration of etomidate in real samples detected by LC/MS and **EtoChrom**, respectively

Real sample	LC/MS Concentration of ET (mg mL^{-1})	**EtoChrom**
1	147.0 ± 0.4	138.7 ± 1.1
2	168.3 ± 0.7	161.7 ± 0.9
3	118.3 ± 0.2	115.7 ± 1.7
4	0	0

2.7. *In situ* detection of etomidate

Recently, an increasing number of criminal cases involving the illegal addition of etomidate to vape juice in E-cigarettes.[5,6] Hence, we would like to verify the feasibility of using **EtoChrom** to detect ET in real samples, which can potentially assist police inspections in the future. The concentrations of ET in four real samples, including three suspected ET-containing samples (samples 1–3) and one commercially available nicotine-containing vape juice sample (sample 4), were first determined *via* LC/MS analysis (Fig. S13†). **EtoChrom** was then used to treat with these samples and their absorption spectra were monitored and compared (Fig. S14†). The corresponding ET concentrations in real samples determined by both methods are summarized in Table 1. From the LC/MS results, samples 1–3 contained *ca.* 147, 168, and 117 mg mL^{-1} ET, respectively, while sample 4 was ET-free. **EtoChrom** exhibited similar results and a pale-yellow colour could also be observed visually for the positive result (Fig. S15†). For quantitative analysis, using the calibration curve shown in Fig. 3d and considering the dilution factor, samples 1–3 were found to contain *ca.* 139, 162, and 116 mg mL^{-1} ET, respectively, with the results lower than those of the LC/MS analysis but within an acceptable error range of *ca.* 5%. Nevertheless, it is illegal to possess any amount of this dangerous drug,[6] and thereby **EtoChrom** can still provide important information despite its upper and lower detection limits being relatively narrow when compared with other reported non-chromatographic methods (Table S2†).[10,11,16] Accordingly, **EtoChrom** can still be considered as an acceptable tool for rapid on-site ET detection because of its advantages such as low cost, no requirement for instruments, matrix treatment-free operation, and easy and fast result reading.

3. Conclusions

In summary, we have developed a novel colorimetric etomidate sensor, **EtoChrom**, based on the $[Cr(H_2O)_6]^{3+}$ complex, utilizing the properties of a bathochromic shift in absorption wavelength and thus the colour change from purple to greenish yellow upon etomidate binding and aqua ligand displacement on the chromium(III) ion as the key principle supported by computational calculation of the monodentate and mono-coordinated geometry. **EtoChrom** can detect etomidate within 1 min with a low detection limit of 0.030 mg mL^{-1}, can provide qualitative and quantitative results up to 2 mg mL^{-1},

unaffected by the common interference species in the vape juice and saliva matrices, and is highly stable for up to 90 days. The highly accurate results with easy-to-read colour change by the naked eye in etomidate-containing real sample analysis renders **EtoChrom** a cost-effective, rapid, easy-to-handle, highly sensitive and etomidate-specific testing kit for practical on-site etomidate detection in vape juice samples.

Author contributions

Leo K. B. Tam: writing – original draft, investigation, formal analysis, data curation, and conceptualization. Weijun Ma: data curation. Boyang Li: data curation. Waygen Thor: investigation, formal analysis, and data curation. Ho-Fai Chau: writing – review & editing. Ka-Leung Wong: writing – review & editing, supervision, project administration, funding acquisition, and conceptualization.

Conflicts of interest

There are no conflicts to declare.

Data availability

The data that support the findings of this study are available in the ESI† of this article.

Acknowledgements

All experiments were performed in compliance with the relevant laws and institutional guidelines of Hong Kong Polytechnic University, according to which human serum albumin (HSA) was purchased and the samples were supplied by Sigma-Aldrich. Financial assistance from the HK PolyU Research Grant No. P0054517 and 4-68AS is gratefully acknowledged (K.-L. W). We thank the Hong Kong Hospital Authority, Pamela Youde Nethersole Eastern Hospital, Narcotics Bureau, Hong Kong Police Force, and the Hong Kong Government Laboratory for their assistance. Inspiring discussions with Dr Chen Xie and Dr Yan-Ho Fung are also highly appreciated.

References

1 G. Zheng, Y. Chen, G. Wu, T. Song, X. Zou, Q. Nie and P. Zhang, *Int. J. Toxicol.*, 2024, 1–9.
2 L. C. McPhee, O. Badawi, G. L. Fraser, P. A. Lerwick, R. R. Riker, I. H. Zuckerman, C. Franey and D. B. Seder, *Crit. Care Med.*, 2013, **41**, 774–783.
3 Y. Feng, X. B. Chen, Y. L. Zhang, P. Chang and W. S. Zhang, *Eur. Rev. Med. Pharmacol. Sci.*, 2023, **27**, 1322–1335.
4 H. Zhang, A. Wu, X. Nan, L. Yang, D. Zhang, Z. Zhang and H. Liu, *Mol. Pharmaceutics*, 2024, **21**, 5989–6006.
5 Notice from the National Medical Products Administration and the National Health Commission of China on Strengthening the Management of Etomidate and Modafinil Pharmaceuticals. Available at: **https://www.nmpa.gov.cn/xxgk/fgwj/gzwj/gzwjyp/20231007154014186.html**.
6 Press release from the Government of the Hong Kong Special Administrative Region on Orders to amend the Dangerous Drugs Ordinance and Control of Chemicals Ordinance to be gazetted on February 14 and etomidate to become a dangerous drug on the same date. Available at: **https://www.info.gov.hk/gia/general/202502/12/P2025021100159.htm**.
7 Y.-K. Jung, S. Y. You, S.-Y. Kim, J. Y. Kim and K.-J. Paeng, *Molecules*, 2019, **24**, 4459.
8 Y. J. Park, E. Cho, S. H. Kim, H. Lee, H. Jegal, M. Park, S. Choe, Y. E. Sim, S.-H. Baek, K. M. Kim and J. Pyo, *J. Forensic Sci.*, 2022, **67**, 2479–2486.
9 T.-F. He, H.-H. Zhu, X.-W. Lin, Y.-Y. Tian, L.-M. Sun, X. Guan, H.-Y. Zhang, L. Tan and S.-C. Wang, *J. Pharmacol. Toxicol. Methods*, 2024, **125**, 107490.
10 Y. Zhao, Y. Guo, Z. Xu, T. Lv, L. Wang, M. Li, X. Chen, B. Liu and X. Peng, *Chem. Commun.*, 2024, **60**, 4691–4694.
11 J. Li, J. Ling, Z. Cai, Y. Liao, P. Xing, W. Liu and Y. Ding, *Forensic Sci. Int.*, 2024, **361**, 112136.
12 E. Garrido, L. Pla, B. Lozano-Torres, S. El Sayed, R. Martínez-Máñez and F. Sancenón, *ChemistryOpen*, 2018, **7**, 401–428.
13 H. Chu, L. Yang, L. Yu, J. Kim, J. Zhou, M. Li and J. S. Kim, *Coord. Chem. Rev.*, 2021, **449**, 214208.
14 V. Kumar, P. Kumar, A. Pournara, K. Vellingiri and K.-H. Kim, *TrAC, Trends Anal. Chem.*, 2018, **106**, 84–115.
15 Y.-H. Shin, M. T. Gutierrez-Wing and J.-W. Choi, *J. Electrochem. Soc.*, 2021, **168**, 017502.
16 Q. Liu, X. Xu, L. Liu, A. Qu, C. Xu and H. Kuang, *Analyst*, 2025, **150**, 542–551.
17 S. Dengl, C. Sustmann and U. Brinkmann, *Immunol. Rev.*, 2016, **270**, 165–177.
18 Y. Mo, X. Zhang, K. Zou, W. Xing, X. Hou, Y. Zeng, Y. Cai, R. Xu, H. Zhang and W. Cai, *Nanomaterials*, 2024, **14**, 1958.
19 S. Rasheed, M. Ikram, D. Ahmad, M. N. Abbas and M. Shafique, *Microchem. J.*, 2024, **206**, 111438.
20 T. Koppanyi, J. M. Dille, W. S. Murphy and S. Krop, *J. Am. Pharm. Assoc.*, 1934, **23**, 1074–1079.
21 M. J. de Faubert Maunder, *Analyst*, 1975, **100**, 878–883.
22 D. F. Shriver, P. W. Atkins and C. H. Langford, *Inorganic Chemistry*, W. H. Freeman and Company, New York, 1994.
23 M. Uchikoshi, D. Akiyama, K. Kimijima and K. Shinodac, *RSC Adv.*, 2022, **12**, 32722–32736.
24 D. Lazar, B. Ribár, V. Divjakovic and Cs. Mészáros, *Acta Crystallogr., Sect. C: Cryst. Struct. Commun.*, 1991, **47**, 1060–1062.
25 Price of chromium(III) nitrate nonahydrate offered by Dieckmann (Hong Kong) Chemical Industry Co. Ltd. Available at: **https://www.dkmchem.hk/product/213963.html?goodsno=MC01913-500g**.

26 R. J. Sundberg and R. B. Martin, *Chem. Rev.*, 1974, **74**, 471–517.
27 J. Reedjik, *Recl. Trav. Chim. Pays-Bas*, 2010, **88**, 1451–1570.
28 J. F. Perez-Benito and X. Julian-Millan, *React. Kinet., Mech. Catal.*, 2019, **128**, 1–22.
29 M. J. Bjerrum and J. Bjerrum, *Acta Chem. Scand.*, 1990, **44**, 358–363.
30 D. Rai, B. M. Sass and D. A. Moore, *Inorg. Chem.*, 1987, **26**, 345–349.
31 S. J. Leach and H. A. Scheraga, *J. Am. Chem. Soc.*, 1960, **82**, 4790–4792.
32 A. J. Muñoz, R. V. Alasino, A. G. Garro, V. Heredia, N. H. García, D. C. Cremonezzi and D. M. Beltramo, *Pharmaceuticals*, 2018, **11**, 47.
33 E. J. Z. Krüsemann, A. Havermans, J. L. A. Pennings, K. de Graaf, S. Boesveldt and R. Talhout, *Tob. Control*, 2021, **30**, 185–191.
34 S. P. Humphrey and R. T. Williamson, *J. Prosthet. Dent.*, 2001, **85**, 162–169.
35 J. G. Allen, S. S. Flanigan, M. LeBlanc, J. Vallarino, P. MacNaughton, J. H. Stewart and D. C. Christiani, *Environ. Health Perspect.*, 2016, **124**, 733–739.
36 P. Kubica, *Molecules*, 2023, **28**, 4425.
37 M. Li, B. Lin and B. Zhu, *Toxics*, 2024, **12**, 884.
38 F. Neese, *Wiley Interdiscip. Rev.: Comput. Mol. Sci.*, 2012, **2**, 73–78.
39 F. Neese, *Wiley Interdiscip. Rev.: Comput. Mol. Sci.*, 2018, **8**, e1327.